A Hybrid Learning Algorithm for Automatic MRI Segmentation of Neurodegenerative Diseases

ISSN (e) 2520-7393
ISSN (p) 2521-5027
www.estirj.com

Naz Memon[1], Ahsan Ansari[2], Sanam Narejo[3]

[1] *Department of Information Technology Engineering MUET Jamshoro.*

Abstract: Due to the relationship of various neurological illnesses with distinct regions of the brain, automated brain segmentation is an active study domain to aid medical practitioners in prognostics and diagnoses. Various technologies for automated brain segmentation have been developed using traditional methodologies such as atlas-based and pattern recognition-based methods. Deep learning approaches have recently outperformed traditional state-of-the-art methods and are gradually maturing. As a result of its ability to understand the detailed properties of high-dimensional data, deep learning has been widely used as a method for exact segmentation of brain areas. This paper proposes a network for segmenting multiple brain areas that is built on 3D convolutional neural networks and uses residual learning and dilated convolution operations to learn the end-to-end mapping from MRI volumes to voxel-level brain segments effectively. The segmentation of up to nine brain areas, including cerebrospinal fluid, white matter, and grey matter, as well as their sub-regions, is the subject of this study.

Keywords: *WM, GM, CSF, ND, AD, MCI, CNN, MRI.*

1. Introduction

There are brain lesions known as White Matter Hyper intensities (WMHs) that present as areas of enhanced brightness on FLAIR sequences of Magnetic Resonance Imaging (MRI). WMH lesions have been associated to cognitive decline, stroke risk, dementia, and other geriatric disorders because of their vascular origin [1]. Brain injury and the associated cognitive and physical disorders can be better understood by utilizing an accurate and exact segmentation process to study the lesions on these types of images. This procedure could also give benchmarks for early detection of the disease [2].

Since so much research is now being done on the human brain, it's generally recognized as the most significant organ for seeing potential health problems before they even occur. When making predictions, many test methods like computed tomography (CT), positron emission tomography (PET), electroencephalograms (EEG) and magnetic resonance imaging are used [3], [4]. Magnetic fields of 1 to 7 Tesla are used in MRI scans. Free hydrogen nuclei align in the direction of the magnetic field when it is applied in a directed phase to a region of interest. The radio signals released by the protons are measured to obtain resonances, which are then converted to MR pictures [5]. The limbic system and diencephalon under the temporal lobe of the brain play an important part in health measurements in the brain, which is considered a complex structure of the human body. Among the parts of the brain that make up the diencephalon are the hippocampus, pituitary gland, olfactory cortex, thalamus, amygdala and hypothalamus, among others. Observation is impossible due to the complexity of these small, asymmetrical structures [6].

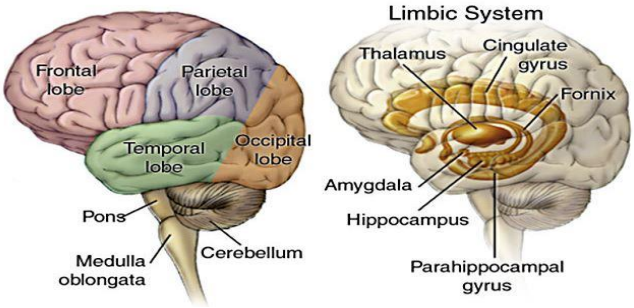

Figure.1 Neurodegenerative Disorders

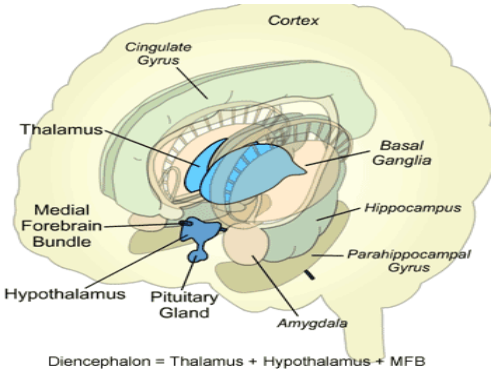

Figure.2 Hypothalamus Disorders

It is a neurodegenerative illness if it results in one or more of these. Studies suggest an uncertain connection between these disorders and the resultant changes in the diencephalon and limbic systems of the human brain, according to a number of investigations. The cells in these regions of the brain deteriorate often. Cell deterioration is measured by atrophy. It's possible to see these alterations on MRI pictures [7], [8].

Corresponding author Email address: *naz.memon85@gmail.com*

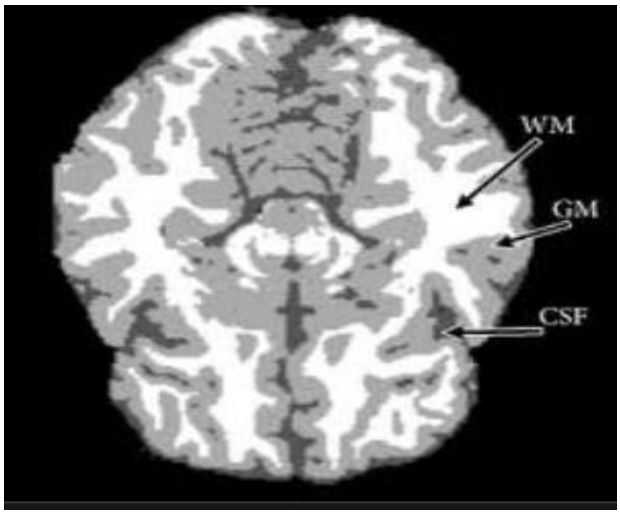

Figure.3 Example of Image taken from Dataset [3]

Tumor identification, tumors segmentation, organ and multi-organ segmentation are all tasks that fall under the medical imaging analysis domain. Since it aids in the detection, diagnosis, and treatment of organ or tissue-related issues, segmentation has become known as one of the major problems in this area [9], [10]. Different brain regions and tissues must be precisely segmented before neurological problems can be detected and diagnosed. The significance of brain segmentation is demonstrated by the fact that conferences such as MICCAI [11], [12] regularly conduct competitions for it. To find the most accurate findings, numerous ways have been tried throughout the years, and even now it remains a difficult process. Because manual segmentations are time intensive and prone to error, scientists are working to develop automated methods. At first, segmentation problems were generally dealt with using atlas-based segmentation or pattern-recognition approaches [13], [14]. Atlas-based approaches use a pre-defined atlas for a certain job and map the image to that atlas.

Despite the fact that atlas-based approaches produce strong segmentation results and are often resistant to anomalies, their reliance on population-specific atlases may limit their applicability to datasets that are not well represented by the atlas [15], [16]. As a result, it's more difficult to precisely separate different types of brain tissue. Atlas-based approaches, on the other hand, are ineffective when the dataset's patient population differs greatly from the atlas. Because of the wide range of brain morphologies among patients, many methods fall short in this situation. Several pattern recognition algorithms have been developed to circumvent these restrictions, including those that leverage spatial, intensity, or other atlas space information as characteristics for the segmentation of various regions. These methods call for certain data or features to complete the job at hand.

Researchers are turning to deep learning architectures because manual, atlas-based, or pattern recognition-based segmentation methods have their limits. Self-learning and generalizable segmentation algorithms based on deep learning [17], [18] are available. Traditional state-of-the-art methodologies are rapidly being surpassed by deep learning systems as they mature. Deep learning algorithms depend on the availability of training datasets to generalize their results. Convolutional Neural Networks (CNN) have shown beneficial in a variety of computer-vision applications, including but not limited to image identification, object detection, classification, and segmentation.. There are no preexisting features or geographical information needed for CNNs because they learn the features in a hierarchical fashion through numerous convolutions over several layers. Through training, the convolutional layers learn about spatial spacing and generalizability [19], [20]. As a result, researchers have utilized CNNs to separate brain areas based on modifying the design of the network according to the job. Three key brain regions have been identified using deep learning methods: Cerebrospinal Fluid (CSF), Gray Matter (GM), and White Matter (WM) (WM). Many other CNN variations have been used to segment many different sub-regions, such as 8, 25, 134, etc. [21], [22]. While deep learning has been widely employed for two-dimensional images, 3D CNNs have emerged as the newest solution for medical imaging segmentation challenges as images are obtained in three-dimensional volumes [23], [24]. When using 2D patches of these volumes, the spatial information contained in 3D photos is lost. Hence for segmentation of three and nine brain regions comprising WM, GM, CSF and their sub-regions this paper [25] provides a deep learning technique using 3D CNN.

2. Related Work

Segmenting the amorphic regions especially in 3 Dimensional plane is demanding phase to be done. Most of the MRI datasets provides only T1-weighted mages that are less revealing for such small ROI [26], [27]. Hence obtaining a T2-weighted images dataset is one of the basic requirement. Manual or Semi-automated segmentation is easy to implement but requires a lot of time and provides less accuracy. Consequently we are aiming for the fully automatic segmentation of Human Brain [28]. The patient's MRI does provide some hidden information according to their disease types, subsequently a remarkable change in a Healthy Brain versus the patient's brain is possible. Most of the time this change is considered in means of lesions, variation in voxel densities or volumetric measures. Some particular segments of hippocampus, hypothalamus or amygdala can provide a noticeable information in neurodegenerative diseases according to D. Louis Collins [29]. The name of his publication is "Towards accurate, automatic segmentation of the hippocampus and amygdala from MRI by augmenting ANIMAL with a template library and label fusion". His research yields the optimal median Dice kappa of 0.866 with the ANIMAL software [30].This section explains the previous work conducted on Neurodegenerative Disorders. Also summarize the research work in a tabular form.

Gan et.al [3] present an automated method for segmenting the cerebral ventricle in 3D MRI scans of the human brain. This method uses a Bayesian framework and a cutting-edge super-pixel plan to precisely segment the lateral ventricle of an MRI scan. Comparing the proposed method's segmentation results with expert manual delineation yielded statistically significant differences. Because of the positive outcomes, this method could be used in clinical studies involving ventricle morphometry.

Nagaraj et.al [8] proposed approaches that were used to evaluate and train the prior image, which was known as the

Gray Level Co Matrix (GLCM). These qualities are put to the test using a neural network to see if they are linked with anything like Parkinson's or schizophrenia. The Support Vector Machine is the preferred neural network (SVM).

Veerman et.al [5] analyses correlations of the atrophy rate between hippocampus and ventricles, four new correlation parameters are introduced. A seven-dimensional vector is created by adding these three global atrophy rate parameters to three local atrophy rate parameters. With the help of various vector classification methods, we examine the method's ability to distinguish AD patients from healthy (NL) controls in 31 longitudinal MRI baseline images and their subsequent follow-ups from the ADNI database. It turns out that the classification results we get and the real-world data agree remarkably well. Accessibility of the analysis has been improved with a custom graphical user interface.

Jiang et.al [19] proposed approach to conduct coarse registration. An algorithmic combination of maximum cross-section area detection and the generic Hough transform is used to achieve fine tuning. The magnetic resonance and scanning electron microscopy (MR/SPECT) images were registered with the help of CT images generated from SPECT CT scans in this investigation. The MR image's outline of the brain's structure might be transferred onto the SPECT image and placed in the proper area in the brain. In two clinical datasets, the accuracy of registration has improved when compared to the results obtained using conventional primary axes alignment alone, which was previously the case. This improvement can be attributed to the use of a more sophisticated registration algorithm.

Leon et.al [7] proposed a data-driven technique compares three PHOW (Pyramid Histograms Of Visual Words) description variants to classify AD. For this study, researchers used the OASIS dataset, which included 87 problematic patients and 87 healthy controls. There was a growth of 27.1% compared to a naive technique with the greatest results at 89.3%, which is currently an AD categorization level. In terms of variety, healthy controls outperformed mentally ill ones by a wide margin (94.5% compared to 84.0%), although early-onset AD patients and elderly controls had the most difficulties. And last but not least, a review of dictionary words revealed a few defining surface traits. The distribution of words globally appears to have a greater impact on local patterns than the location of the word itself for purposes of classification.

Couty et.al [9] used techniques to diagnose and monitor tumours and neurological diseases. Despite the fact that these coils are flexible and wireless, they are easy to manufacture in huge quantities with little effort. Aside from that, we present the results of the first inquiry into the effects of packaging on the characteristics of the coil, such as the f0 and the Q factor. The use of PDMS to enhance the packaging has allowed us to capture the first in vivo image of the rat brain using an implanted flexible micro antenna, which was previously unattainable due to the complexity of the packaging.

Abdulkadir et.al [11] Proposed model that generates maps of expected GM densities and displays them as a function of location. Map GM densities were adjusted to be lower than the actual GM densities in order to prevent classification confusion. Mild cognitive impairment patients were compared to stable MCI patients, patients with Alzheimer's disease were compared to age-matched controls, patients with pre-manifest HD were compared to controls, and patients with manifest HD were compared to age-matched controls in four classification tasks. Although the recommended strategy boosted classification accuracy in most cases, it had no net effect on accuracy. The confounding effects were decreased by using kernel linear regression, and the outcomes remained the same.

Tosun et.al [20] proposed that only significant connections existed only in the right side of the brain. When compared to controls, multimodality revealed the most significant atrophy and hyper fusion in the brain. A small multimodality effect size was found in areas identified by unimodality analysis of atrophy and hyper-fusion differences compared to patients with brain vascular disease (bvFTD) and healthy controls. JICA’s ability to interpret multimodality brain imaging data effectively was found in these findings.

Burgess et.al [12] proposed a new technique for non-invasively transferring neural stem cells to the brain. Magnetic resonance imaging (MRI) broke down the blood-brain barrier by focusing on the striatum and hippocampus on the left (BBB). Definity microbubble contrast agent was administered intravenously before the sonication procedure began. After the BBB was damaged, GFP-expressing neural stem cells were injected into the carotid artery. MRI and routine post-mortem immunohistochemistry discovered the cells while they were still alive in the body. Images with contrast enhancement were used to determine whether FUS increased BBB permeability.

The cells had crossed the BBB and were found in the left striatum and hippocampus, according to immunohistochemistry. 24 hours after sonication, GFP-positive cells exhibited a neuronal phenotype and high levels of nestin, polysialic acid, and doublecortin expression. Studies have shown that magnetic resonance imaging (MRIgFUS) is an effective tool for guiding FUS (MRIgFUS) cell delivery. In the future, this technique may help to reduce the risks of cell transplantation while also improving the effectiveness of clinical stem cell treatments.

Gal et al. [1] proposed the features extracted from segments of white matter (WM), grey matter (GM), and cerebrospinal fluid (CSF) samples were fed into a convolutional neural network (CNN) to determine the cause of the disease (CNN). Principal component analysis (PCA) can be used to extract a relevant feature set for daily life, moderate cognitive impairment (MCI), and Alzheimer's disease (AD) from the deep sections acquired by principal component analysis. Support vector machines (SVMs) are pretty useful (SVM). According to the study's findings, GWO based on Stalls is capable of reliably segmenting normal, MCI, and AD tissues with high accuracy while maintaining the so called reliability.

Table.1. Comparative Analysis

Reference	Dataset	Technique	Outcomes	Accuracy
Li et al [2]	(rs-fMRI) brain	Deep Neural Networks	Alzheimer's and Parkinson's patients.	89%
León et al [7]	OASIS Dataset	Deep Neural Networks	Alzheimer's and Parkinson's patients.	89.4%
Burgess et al [12]	Brain Dataset	FUS	striatum and hippocampus disorders detection	91%
Wang et al [13]	Brain Dataset	CNNs, MLPs	detect Alzheimer's disease and dementia	88%
Abdulkadir et al [14]	ADNA	Gaussian Models	Alzheimer's disease	87.5%
Goyal et al.[15]	(rs-fMRI) brain	Deep Neural Networks	Neurodegenerative Disorders	Accuracy 76.7% for WM and 80.22% for CSF
Lei et [16]	ADNA	Gaussian Models	Alzheimer's disease	84.78%
El-Gamal et al.[17]	Brain Dataset	DenseNet	detect Alzheimer's disease and dementia	86%

Goyal et al. [15] proposed in-depth features of detecting discrimination in the data. As a result of the classifier, distinct tissue differences can be observed between healthy individuals, those with mild cognitive impairment, and those with dementia. Accuracy is scored at 76.7 per cent for WM and 80.22 per cent for General Motors and Central Science and Technology (CSF). In comparison to the effects of time and age, genetic variation is the biological substrate that most closely correlates with the progression of dementia. By employing the framework that has been proposed thus far, it is conceivable to construct a diagnostic strategy for the advancement of neurodegenerative diseases in the future.

Cheng et al [2] proposed that Parkinson's disease (PD) results in decreased brain connectivity, particularly in the areas responsible for movement and memory. Scientists monitored Z scores to see if connectivity was being disrupted as the disease progressed. Researchers have discovered abnormalities in brain networks in Alzheimer's and Parkinson's patients who had functional connectivity in their brains while asleep (rs-fMRI). In brain network topology research, theoretical graph modelling is widely used. As Alzheimer's disease advances, researchers found that connectivity in brain regions associated with motor and memory declines. The motor and memory areas of the brain lose connectivity in Parkinson's disease (PD). In addition, the decreasing Z scores in the diseased areas show a decrease in connectivity over time in Alzheimer's and Parkinson's patients.

Wang et al. [13] proposed strategy has been recommended as an alternative to the traditional method since it is more efficient, less expensive, and more reliable than the latter. Authors believe that deep learning is the most advanced form of artificial intelligence currently available. Image processing is more accessible thanks to Convolutional Neural Networks (CNNs) inspired by biology, also known as multilayer perceptions, making image processing more accessible (MLPs). Using 3D magnetic resonance imaging data, the researchers developed a state-of-the-art Deep Convolutional Neural Network to detect Alzheimer's disease and dementia.

Farooq et al. [10] present a method for assisting neurologists in assessing anatomical and functional changes in cerebral structure from MRI scans of neurological patients that uses grey and white matter segmentation from patient brain MRI slices to aid in determining anatomical and functional changes in cerebral structure. It is planned to use this approach in the development of a computational software platform. The preceding section demonstrated how the software could be integrated into a hospital's computational media for neurology.

Sinatra et al. [6] Concentrated on segmenting 6-month-old infant brain images. Its goal is to enhance methods and encourage community participation in the sector. These metrics were used to rank the best eight clubs in Sieg-2017. Authors also introduced their pipelines, source codes, and implementations. Authors also talk about problems had and remedies. The Sieg-2017 dataset and this review article may help the research community grow methodologically.

Zhang et al. [30] used Brain image classification to identify Alzheimer's disease (AD), Parkinson's disease (PD), and other forms of dementia through detection, prediction, and diagnosis. Atrophy of the brain occurs as a result of neuronal cell degeneration in neurodegenerative disease. Detection and treatment of neurodegenerative diseases (ND) such as Alzheimer's disease are most effective when done early on. Detection and diagnosis of neurodegenerative diseases using computer vision.

Huang et al. [16] investigates whether metal compounds found in neurodegenerative diseases can be measured with it (including SQUID sensors). This approach has resulted in simple diagnostic devices that can detect multiple concentrations of well-known ferromagnetic compounds concentrated in a single localized area, with promising results so far in the lab.

Barnes et al. [4] Proposed SC U-net outperformed two other approaches, one of which uses deep learning to improve segmentation accuracy. Our SC U-superior net's performance was assessed on a quantitative and qualitative basis (visual examinations). This proposal's average dice score was 78.36%, significantly higher than a U-net-like method (74.99%) or an alternative deep learning method (74.80 percent). The proposed system's software environment and model are hosted on the Docker hub.

3. Methodology

A combination of multiple techniques are sometimes proved to increase the efficiency of algorithms. A completely noise free MRI images can be obtained by applying one of the suitable noise filter. These images then could be segmented using various algorithms. A hybrid approach that incorporates positive measures of more than one algorithms and reduces the processing time can be proposed. Clustering techniques as Fuzzy logics incorporated with brain Masks and atlases are expected to provide better results. Once the MRI is segmented. Validation phase can be completed by comparing the segmented MRI with provided ground truths. The Validated image by overlapping with the healthy control subject's MRI would be revealing some crucial information about the patients. As the tissue densities, lesion detection or atrophy measures. These could be observed in the resulting images.

The main contribution to this study are:

- Segmentation of Brain Magnetic Resonance Images
- Proposing a Hybrid Algorithm
- Increasing the Efficiency of Segmentation algorithms.
- Analyzing the difference between healthy control MRI and the patients.
- Calculating the brain atrophy measures.
- Detection of lesions.

3.1. Dataset

This research collected data from the skull stripped database of the Alzheimer's Neuro-imaging initiative. Skull stripped is a global programme that provides correct scientific evidence in pathogenesis theory, AD prevention and therapeutic trials. Many study classes contribute to the understanding of the development of AD in a human brain by studying biological markers. This dataset will assist us to detect Alzheimer's disease progression. This dataset comprises Hippocampus gland MRI segmentation. There are two portions. There are two. The first half includes photographs of 100 people as train data, while the second part includes images of 35 people as test data. All pictures are for Alzheimer's sufferers.

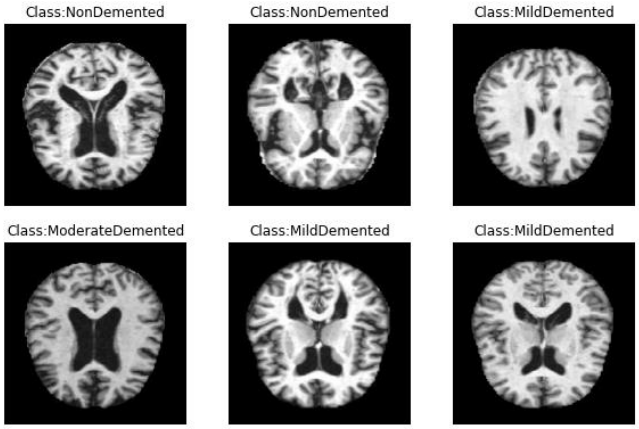

Figure.4 Samples from Dataset

3.2. Ground truths

SRI124 Package: An MRI-based atlas of normal adult human brain anatomy, created using nonrigid registration from scans of 24 normal control participants, is known as SRI24. All of this information is contained in a single atlas that includes T1, T2, and DTI-weighted structural images of the brain, as well as maps of cortical areas and subcortical structures that can be labelled with two different sets of identifiers (cortical regions and subcortical structures). The atlas is given in Analyze, NIFTI, and Nrrd formats with a 1mm isotropic image resolution. In addition, we're offering SPM8 users an experimental package.

3.3. 3D-UNets Model with ResNet Ecnoder (Hybridization).

A U-Net is a deep convolutional neural network architecture designed for the segmentation of biomedical images. For tasks where the output is close in size to the input and output requires the spatial resolution, U-Nets were detected to be quite efficient. This makes them ideal for segmentation masks and image processing/generation including super-resolution or colorization.

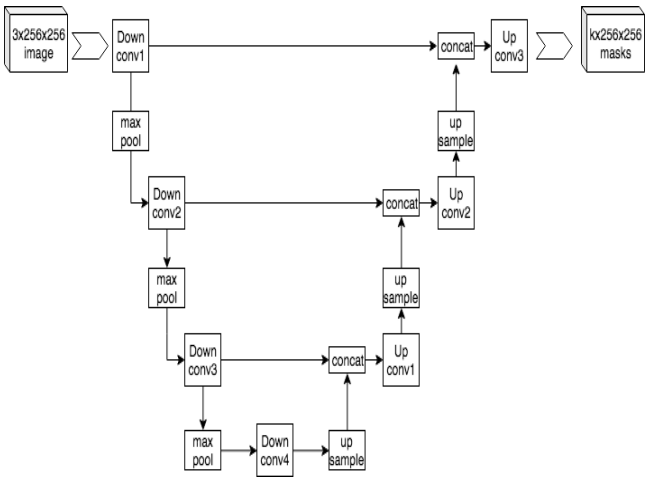

Figure.5 Proposed Architecture of UNets with Up-sample and Down-sample of COnv2D layers

When convolutional neural networks are widely used in classification pictures, the picture is taken and sampled in one or more classifications using a set of two steps, reduced each time the grid scale. To produce a picture of the same size as the input, or larger, a sampling path must be provided to increase the grid size. The architecture of the network is

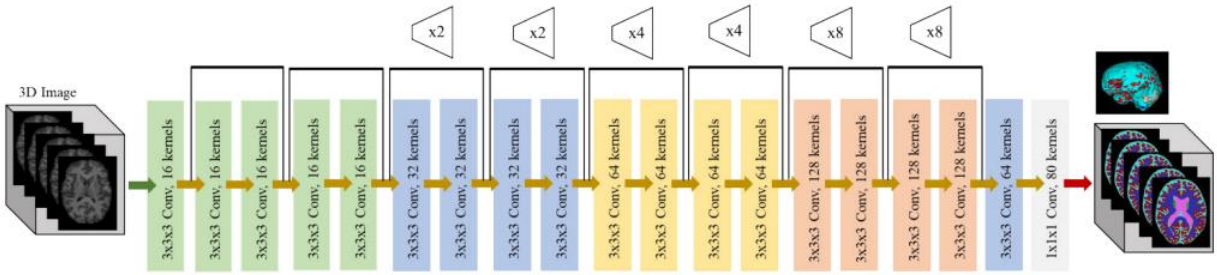

Figure.6 Proposed Methodology Working

like the U shape, a U-Net the down sample/encoder path forms the left side of the U and the up sample/decoder path forms the right half of the U.

This is achieved by multiple transposed convolutions for the Up sample/decoder direction, each inserting pixels between and around established pixels. The down sampling direction is essentially reversed. The alternatives for up sampling algorithms are further explored. Notice that there are often cross links in this model's U-Net architecture that are more comprehensive, these were not part of the initial U-Net architecture.

a. Upsampling/ transposed convolutions

To achieve the required resolution, any Upsample in the decoder/Upsample part of the network (right hand part of the U) should add pixel around the current pixels and also between the existing pixels. This method can be seen from the paper "Guide to deeper learning convolution arithmetic," which includes zeros within pixels. The initial 2x2 pixels are blue pixels, which are extended to 5x5 pixels. 2 pixels of padding are applied to the exterior and a pixel between each pixel is also added. All new pixels are 0 in this case (white).

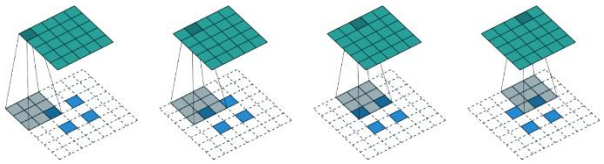

Figure.7 Up sample of Transposed CNN

Adding pixels in and around the pixels. This should have been better by using the weighted average pixels (using bi-linear interpolation), by simply initializing the new pixel, as otherwise the learning of the model might have been overly difficult. In these models it employs an enhanced process, known as the pixel shuffle or sub-pixel convolution, which results in a far more efficient filling of gaps between pixels.

b. Pixel shuffle

The pixel shuffle increases by a factor of 2, twice the size of each picture channel (in its current representation at that part of the network). Replication padding is done to supply an additional pixel across the image. Average pooling is then done to remove functionality seamlessly to prevent the pattern of the checker board resulting from several mega resolution techniques. After the representation of these new pixels is introduced, the following convolutions boost the details as the path proceeds along the network decoder path before upgrading another phase and doubling the size.

c. U-Nets and fine image detail

With just one U-Net architecture projections appear to miss information, they can be inserted between network blocks to solve this crossover or to override connections. Rather than inserting a skip link every two turns, as in a ResBlock, the skipping connections are crossed from the same size portion into the sample route. There are the grey lines seen in the above illustration. The original pixels are combined with the final ResBlock with a skip relation, which allows final calculation with knowledge of the original pixels entered into the model. The consequence is that all the input picture information are at the top of the U-Net with the input mapped almost directly to the display. The outputs of the U-Net blocks are more close to the Dense Blocks than to the ResBlocks. But there are two steps that decrease the grid capacity, which also helps prevent memory use from getting too big.

d. ResNet Encoder

For the U-Net encoder/down sampling segment, an inception v3, vgg16 and vgg19 can be used (the left half of the U).

e. Decoder

When given an encoder architecture, the Fastai U-Net learner will construct the decoder side of the U-Net architecture automatically, in this case converting the ResNet encoder into a U-Net with cross-connections.

f. Pre-trained encoder

If a pre-trained algorithm is used to train an image generation/prediction model, it greatly reduces the amount of time it takes to train the model. After that, the model has a basic understanding of the types of functionality that need to be found and changed. Where images are used as inputs, using a model and weights that have been pre-trained on ImageNet is a great place to start.

g. Loss functions

Using a loss function based on activations from a pre-trained model (such as inception v3, vgg16 and vgg19) and gram matrix loss while using this U-Net design for image generation/prediction has proven to be extremely accurate. Loss function can be calculated as:

$$L = \sum_{i=0}^{n} logi + (1 - yi)\log(i - oi) = \frac{2\sum_{i=0}^{n} oiyi}{\sum_{i=0}^{n} oi - \sum_{i=0}^{n} yi} \dots (3.1)$$

Where y is the total true positives and o is the false positive values.

h. Data Splitting

Ultimately, the data has been splitted into training, testing and validation with the ratio of 70%, 24% and 6% respectively. We can split our dataset in any ratio but we used this conventional ratio for the best classification of our model.

Training Dataset: A collection of data which is used to match the model.

Validation Dataset: A collection of data utilized provides an unbiased assessment of the model fit to the testing set when tuning the model hyper parameters. The assessment is more skewed as the expertise on the trained set is integrated into the specified model.

Test Dataset: A sample of data collected to get an unbiased measure of the measurement result fit to the training dataset .

The aim of this research is to provide a fast building image classification pipelines including data Input/Output, preprocessing, data augmentation, patch-wise analysis, metrics, a library with state-of-the-art deep learning models and model utilization like training, prediction as well as fully automatic evaluation (e.g., cross-validation). Our technique is based on Keras with Tensorflow as backend. We have selected 300 images from dataset. The original scans have an image resolution of 512x512 and on average 216 slices (highest slice number is 1059). All the models that are discussed above passed through following preprocessing and classification steps:

i. Raw Image Preprocessing

In general, preprocessing techniques can handle the noise of the images and deep learning techniques learn to avoid these noises while making classification and predictions, though their ability to learn is conditioned upon the availability of large training data. The Deep Learning models are easily susceptible to overfitting. The first step in the pipeline is to establish a Data I/O. It offers the utilization of custom Data I/O Tumor Class for fast integration of your specific data structure into the pipeline. We have used data preprocessing techniques to remove noise and noises on the images. We have modified the noise removal algorithm. The steps include:

j. Conversion into Grayscale

The arrangement of sharpness, shadow, contrasts, and construction of the color picture are novel procedures. To alter the Red Green Blue (RGB) into grayscale, an average method is used.

k. Binary Thresholding

It is a modest procedure of image segmentation. It is a technique to produce a binary image from an RGB image or grayscale. Typically, we use this to separate foreground pixels from the background pixels.

l. Pre-processed Data:

As to validate our model properly, we have pre-processing steps. We create high quality, the balanced dataset for testing and validation as our downloaded dataset was unbalanced. We used to remove noise in pre-processing that was mainly due to bad light, noise, and air bubbles.

m. Append Original Images

When we use the Keras Image Data Generator, we are loading up several slightly altered versions of our original images. Therefore, our training folder contains none of our original images. To complete our dataset, we will now append the original images into the training folder. Furthermore, we will add the images that were set aside for testing and validation into their appropriate folders.

n. Model Building

For classification of dataset images model training and building is used. In the deep networks methods, the first step is to initiate the classification Model. Then we train the model on our training data and find the optimal learning rate.

4. Results & Discussions

Using the 3D UNets and ResNet Encoder, the WM, CSF and GM was segmented in the real 3D MR image series obtained from the patient. As a gold standard, the segmented images were compared to the manually segmented images to ensure that the procedure was accurate and reliable. In the following tables, we have summarized the features that are extracted and volumetric analysis of CSF, GM and WM. Figure below shows the segmented view of 36223:

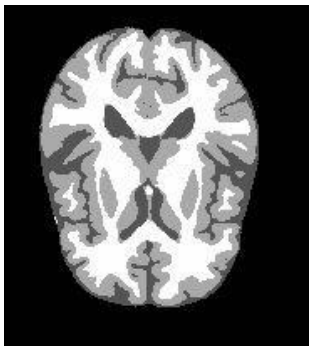

(a) Axial

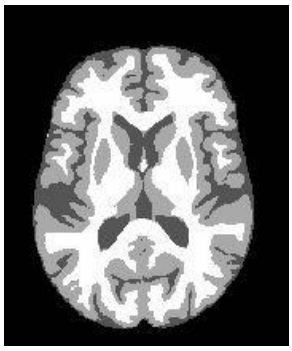

(b) Axial Transverse

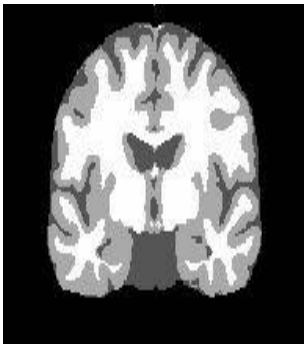

(c) Coronal

(d) Sagittal

Figure.8 Segmentation Alignments

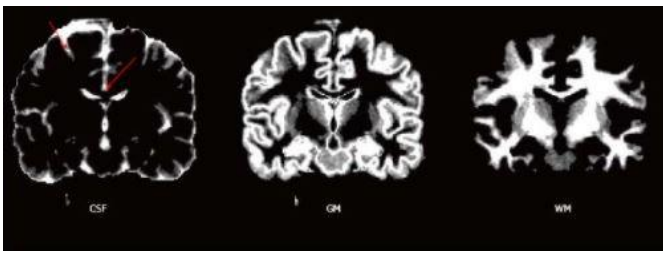

Figure.9 Coronal View

Figures below shows the segmentation of different tissue classes in brain:

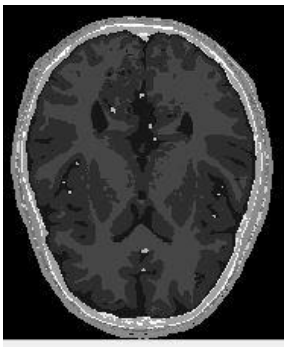

(a) Original

(b) Segmentad Image

(c) Grey Matter

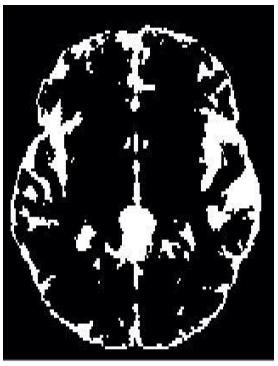

(e) CSF

(f) White Matter

Figure.10 Segmented parts

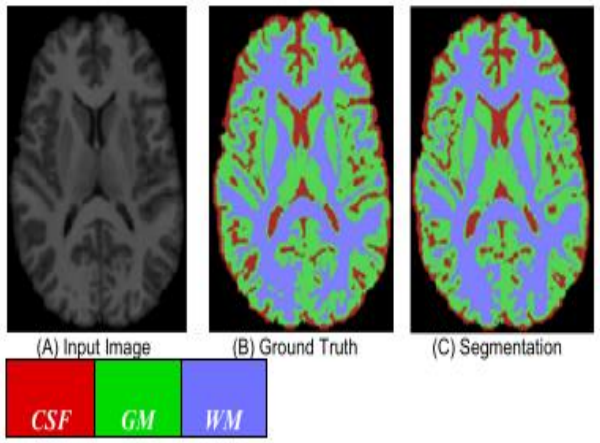

Figure.11 Segmentation in Colored Regions

Figure 11 shows the Input Image, Ground Truth and Segmented Part. Red color shows the CSF, Green shows the Grey matter and Blue shows the White Matter.

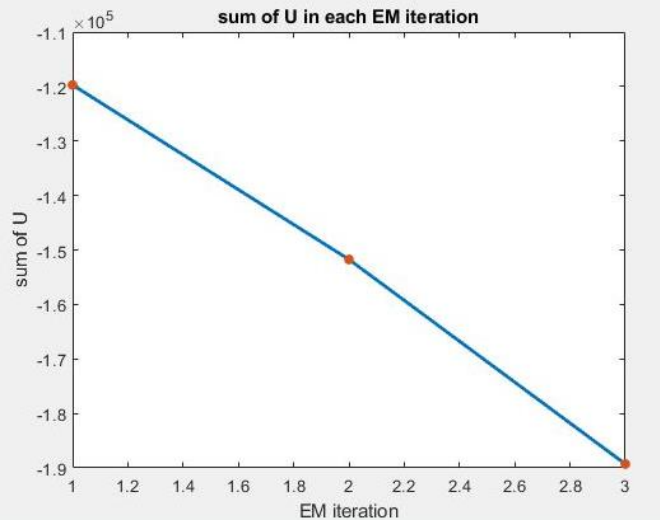

Figure.12 Sum of U in each EM iterations
Figure 12 shows for 3rd iteration the sum of U becomes -1.9x10^5

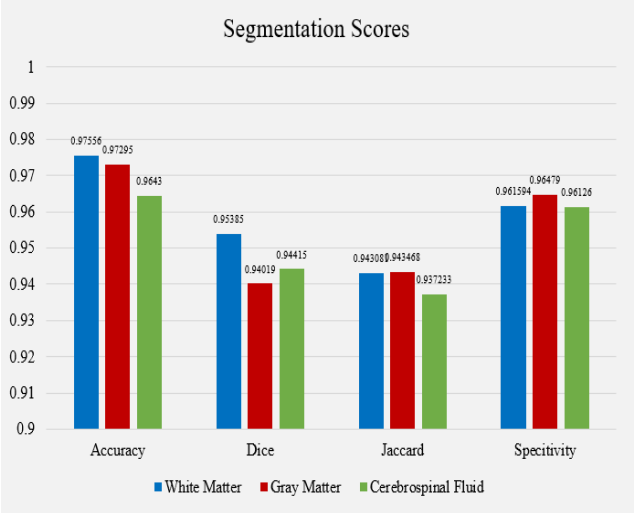

Figure.13 Segmentation Scores
Figure above shows the graphical image segmentation results in the form of accuracy, dice score, jaccard and specificity.

Table.1 Some Examples of random subject's segmented MRI

Dataset Name	Ground Truth	Accuracy	Dice	Jaccard	Specitivity
Subject 36223 - WM	Sri 24_pbmap_WM	0.9744	0.937598	0.902401	0.953414
Subject 36252 - WM		0.9633	0.959598	0.947801	0.978814
Subject 36259 - WM		0.9869	0.945598	0.924742	0.965756
Subject 36230 - WM		0.9604	0.932598	0.917379	0.948393
Subject 36223 - GM	Sri 24_pbmap_GM	0.9532	0.95378	0.900694	0.95361
Subject 36252 - GM		0.9736	0.945781	0.946094	0.97901
Subject 36259 - GM		0.9828	0.928378	0.933035	0.965952
Subject 36230 - GM		0.9822	0.932809	0.914048	0.948589
Subject 36223 - CSF	Sri 24_pbmap_CSF	0.9651	0.954965	0.879053	0.978639
Subject 36252 - CSF		0.9634	0.956968	0.924453	0.973804
Subject 36259 - CSF		0.9727	0.919968	0.921395	0.99098
Subject 36230 - CSF		0.956	0.944684	0.904032	0.973617

5. Conclusion

Medical professionals rely on automated brain segmentation for prognostics and diagnostics because of the correlation between various neurological disorders and certain regions of the brain. Traditional methods such as atlas-based and pattern recognition-based methods have been used to develop several systems for automated brain segmentation. In recent times, deep learning approaches have outperformed more traditional methods, and this trend is expected to continue in the future. Deep learning has been widely employed as a method for precise segmentation of brain areas because of its ability to understand the complex features of high-dimensional input. To efficiently train the end-to-end mapping from MRI volumes to voxel-level brain segments, this research offers a network based on 3D convolutional neural networks that uses residual learning and dilated convolution operations. There are up to nine distinct brain regions that are being studied in this research, including cerebrospinal fluid, white matter, and grey matter, as well as their sub-regions. For separating the brain into different regions such as cerebrospinal fluid, white matter, and grey matter using 3D UNets Model is an important step in brain research. Instead than relying on graph theory or atlas-based techniques for medical image segmentation, this research focused on using a 3D deep learning segmentation algorithm. A 3D CNN-based network was used to segment the third and ninth brain areas in this case..

6. References

[1]. Y. Gal, R. Islam, and Z. Ghahramani, (2017) Deep Bayesian active learning with image data, in 34th International Conference on Machine Learning, ICML, vol. 3, pp. 1923–1932, doi: 10.17863/CAM.11070.

[2]. F. Li, D. Cheng, and M. Liu, (2018) Alzheimer's disease classification based on combination of multi-model convolutional networks, in IST 2017 - IEEE International Conference on Imaging Systems and Techniques, Proceedings,-January, pp. 1–5, doi: 10.1109/IST.2017.8261566.

[3]. DSP 2015 : (2015) IEEE International Conference on Digital Signal Processing (DSP) : 21-24 July 2015, Singapore. .

[4]. IEEE Instrumentation and Measurement Society and Institute of Electrical and Electronics Engineers, IST (2018) : IEEE International Conference on Imaging Systems and Techniques : Kraków, Poland, October 16-18, conference proceedings. .
[5]. IEEE Signal Processing Society and Institute of Electrical and Electronics Engineers, (2012) IEEE International Conference on Image Processing : ICIP 2012
[6]. Politecnico di Torino, IEEE Instrumentation and Measurement Society, and Institute of Electrical and Electronics Engineers, I²MTC (2017) IEEE International Instrumentation and Measurement Technology Conference : 2017 proceedings papers : May 22-25, 2017, Politecnico di Torino, Torino, Italy. .
[7]. R. Mendoza-León, F. A. González, P. Arbeláez, J. Puentes, and M. H. Hoyos, (2016) ANALYSIS OF PHOW REPRESENTATIONS FOR ALZHEIMER DISEASE CLASSIFICATION ON BRAIN STRUCTURAL MRI.
[8]. B. Nagaraj et al., ICIIECS'15 : DRDO sponsored (2015) IEEE International Conference on Innovations in Information, Embedded and Communication Systems : 19th and 20th March 2015 : proceedings. .
[9]. Ieee, (2012) IEEE Topical Conference on Biomedical Wireless Technologies, Networks, and Sensing Systems. IEEE, 2012.
[10]. AISSMS Institute of Information Technology and Institute of Electrical and Electronics Engineers, (2020) International Conference on Emerging Smart Computing and Informatics (ESCI) : AISSMS Institute of Information Technology, Pune, India.
[11]. IEEE Signal Processing Society and Institute of Electrical and Electronics Engineers, PRNI (2014) : International Workshop on Pattern Recognition in Neuroimaging : proceedings : 4-6, Tübingen, Germany. .
[12]. A. Burgess, C. A. Ayala-Grosso, M. Ganguly, J. Jordão, I. Aubert, and K. Hynynen, (2011))Delivery of stem cells to the brain using MRIgFUS, IEEE Int. Ultrason. Symp. IUS, pp. 13–16, 2011, doi: 10.1109/ULTSYM.2011.0004.
[13]. L. Wang et al., "Benchmark on automatic six-month-old infant brain segmentation algorithms: (2019)The iSeg-2017 challenge," IEEE Trans. Med. Imaging, vol. 38, no. 9, pp. 2219–2230, doi: 10.1109/TMI.2019.2901712.
[14]. A. Abdulkadir, O. Ronneberger, S. J. Tabrizi, and S. Kloppel, (2014) Reduction of confounding effects with voxel-wise Gaussian process regression in structural MRI, Int. Work. Pattern Recognit. Neuroimaging, PRNI 2014, pp. 1–4, doi: 10.1109/PRNI.2014.6858505.
[15]. A. Goyal, M. K. Arya, R. Agrawal, D. Agrawal, G. Hossain, and R. Challoo, (2017) Automated segmentation of gray and white matter regions in brain MRI images for computer aided diagnosis of neurodegenerative diseases, IMPACT- Int. Conf. Multimedia, Signal Process. Commun. Technol., pp. 204–208, doi: 10.1109/MSPCT.2017.8364005.
[16]. H. Lei et al.,(2019) Parkinson's Disease Diagnosis via Joint Learning from Multiple Modalities and Relations, IEEE J. Biomed. Heal. Informatics, vol. 23, no. 4, pp. 1437–1449, doi: 10.1109/JBHI.2018.2868420.
[17]. F. E. Z. A. El-Gamal et al.(2018) A cortical based diagnosis system for MCI based on sMRI features fusion," IST 2018 - IEEE Int. Conf. Imaging Syst. Tech. Proc., no. Mci, pp. 1–6, doi: 10.1109/IST.2018.8577127.
[18]. R. Mendoza-león et al., (2012) analysis of phow representations for alzheimer disease classification on brain structural mri systems and computing engineering department, school of engineering , universidad de los andes , lab- sticc umr cnrs 6285 équipe decide , département image et t, pp. 24–27.
[19]. C. F. Jiang, D. S. Chen, and Y. R. Li, (2012) A hybrid registration method for brain image analysis," Proc. - 2012 Int. Symp. Comput. Consum. Control. IS3C, pp. 464–466,, doi: 10.1109/IS3C.2012.123.
[20]. D. Tosun, M. W. Weiner, N. Schuff, H. Rosen, and B. L. Miller, (2010) Joint independent component analysis of brain perfusion and structural magnetic resonance images in dementia, Proc. - Int. Conf. Pattern Recognit., pp. 2720–2723, doi: 10.1109/ICPR.2010.666.
[21]. Z. Sun, J. A. C. Veerman, and R. S. Jasinschi, (2012) A method for detecting interstructural atrophy correlation in MRI brain images, Proc. - Int. Conf. Image Process. ICIP, pp. 1253–1256, doi: 10.1109/ICIP.2012.6467094.
[22]. T. Happila and P. Kingston Stanley,(2015) Brain pattern recognition based classification of neurodegenerative diseases, ICIIECS IEEE Int. Conf. Innov. Information, Embed. Commun. Syst.doi: 10.1109/ICIIECS.2015.7193135.
[23]. K. Gan, (2015) Automated segmentation of the lateral ventricle in MR images of human brain, Int. Conf. Digit. Signal Process. DSP, pp. 139–142, 2015, doi: 10.1109/ICDSP.2015.7251846.
[24]. C. Trigona et al., (2017) RTD-fluxgate sensor for measurements of metal compounds in neurodegenerative diseases, I2MTC IEEE Int. Instrum. Meas. Technol. Conf. Proc, doi: 10.1109/I2MTC.2017.7969672.
[25]. H. M. T. Ullah, Z. A. Onik, R. Islam, and D. Nandi, (2018) Alzheimer's Disease and Dementia Detection from 3D Brain MRI Data Using Deep Convolutional Neural Networks, 3rd Int. Conf. Converg. Technol pp. 8–10, doi: 10.1109/I2CT.2018.8529808.
[26]. Y. F. Khan and B. Kaushik, (2020) Computer Vision Technique for Neuro-image Analysis in Neurodegenerative Diseases:A survey, Int. Conf. Emerg. Smart Comput. Informatics, ESCI pp. 346–350, doi: 10.1109/ESCI48226.2020.9167520.
[27]. A. Kavitha, S. S. Prakash, P. Sreeja, and A. S. Carshia, Investigations on the Functional connectivity disruptive patterns of progressive neurodegenerative disorders, Proc. Annu. Int. Conf. IEEE Eng. Med. Biol. Soc. EMBS, pp. 800–803, doi: 10.1109/EMBC. 8856919.
[28]. N. A. Priyanka and G. Kavitha, (2019) Study of Tissue Variation and Analysis of MR Brain Images using Optimized Multilevel Threshold and Deep CNN Features in Neurodegenerative Disorders, Proc. Annu. Int. Conf. IEEE Eng. Med. Biol. Soc. EMBS, pp. 2773–2776, doi: 10.1109/EMBC.2019.8856498.
[29]. M. Couty et al.,(2012) Implantable wireless microcoils for 7Tesla Magnetic Resonance Imaging of the rat brain: Optimization of the PDMS packaging," RWW 2012 - Proc. 2012 IEEE Top. Conf. Biomed. Wirel. Technol. Networks, Sens. Syst. BioWireleSS, pp. 37–40, doi: 10.1109/BioWireless.2012.6172728.
[30]. J. Wu, Y. Zhang, K. Wang, and X. Tang, (2019) Skip connection U-Net for white matter hyperintensities segmentation from MRI, IEEE Access, vol. 7, pp. 155194–155202, doi: 10.1109/ACCESS.2019.2948476.

About Authors

1. Naz Memon, Master's Student at Department of Information Technology engineering MUET Jamshoro. +923316062606 (naz.memon85@gmail.com)
2. Ahsan Ansari, assistant professor at Department of Computer systems engineering MUET Jamshoro+923332663569 (ahsan.ansari@faculty.muet.edu.pk)
3. Sanam Narejo, assistant professor at Department of Computer systems engineering MUET Jamshoro. +923332805454 (sanam.narejo@faculty.muet.edu.pk)